DeepACC:Automate Chromosome Classification based on Metaphase Images using Deep Learning Framework Fused with Prior Knowledge

Chunlong Luo[1,3], Tianqi Yu[2], Yufan Luo[1,3], Manqing Wang[2], Fuhai Yu[2], Yinhao Li[1,3], Chan Tian[2(✉)], Jie Qiao[2(✉)], and Li Xiao[1(✉)]

[1] Key Laboratory of Intelligent Information Processing, Advanced Computer Research Center, Institute of Computing Technology, Chinese Academy of Sciences, Beijing, China
xiaoli@ict.ac.cn

[2] Peking University Third Hospital, Beijing, China
tianchan_cdc@126.com, jie.qiao@263.net

[3] School of Computer and Control Engineering, University of Chinese Academy of Sciences (UCAS), Beijing, China

Abstract. Chromosome classification is an important but difficult and tedious task in karyotyping. Previous methods only classify manually segmented single chromosome, which is far from clinical practice. In this work, we propose a detection based method, DeepACC, to locate and fine classify chromosomes simultaneously based on the whole metaphase image. We firstly introduce the Additive Angular Margin Loss to enhance the discriminative power of model. To **alleviate batch effects**, we transform decision boundary of each class case-by-case through a siamese network which make full use of prior knowledges that chromosomes usually appear in pairs. Furthermore, we take the clinically seven group criterion as a prior knowledge and design an additional Group Inner-Adjacency Loss to further **reduce inter-class similarities**. 3390 metaphase images from clinical laboratory are collected and labelled to evaluate the performance. Results show that the new design brings encouraging performance gains comparing to the state-of-the-art baselines.

Keywords: Chromosome Classification · Object Detection · Deep Learning Framework Fused with Prior Knowledge

1 Introduction

Chromosome classification is an important stage in karyotyping procedure. Karyotyping [14] is useful for detecting chromosomes abnormalities, including numerical and structural abnormalities which may result in several genetic diseases such as Down syndrome [16]. In clinical practice, cytologists capture chromosomes that appears in the metaphase stage of cell division and use Giemsa staining technique to obtain banding patterns which has obvious unique bands of dark

and light color. Then, cytologists can take advantage of chromosomes characteristics to order chromosomes in a standard format. Normally, a human cell owns 46 chromosomes consisted by 22 pairs of autosomes and 1 pair of sex chromosomes (XY or XX). However, chromosome classification is a highly skilled cytogenetic techniques and well-trained operators always need many years of experiences. Meanwhile, considerable manual effort is required yet to identify various types of chromosomes.

To reduce the burden of cytologists in chromosome classification, there are some computer aided classification methods proposed. Traditional classification methods mostly rely on handcraft features. Ming et al. [13] takes the banding patterns as features which are extracted by averaging gray profile, gradient profile and shape profile and then classified them by multilayer classifier. Markou et al. [12] uses a support vector machine to discriminate chromosomes and take the band-profiles which are extracted along axis as input of classifier. Recently, researchers use deep learning method to solve chromosome classification problem and obtain decent performances. Sharma et al. [20] firstly applies some preprocessing on chromosomes segmented through crowdsourcing and then classify them using CNN network. Gupta et al. [21] also uses pre-processing algorithm for bent chromosomes and then employs Siamese Network to extract discriminative embeddings for the final Multi-layer Perceptron classifier. Qin et al. [17] extracts global-scale features and local-scale features using varifocal mechanism and concatenates both above features to predict type and polarity simultaneously.

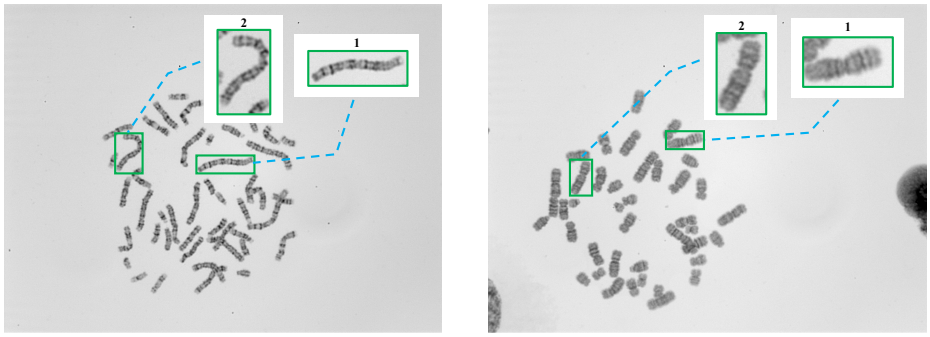

Fig. 1. Two metaphase images show classification difficulty caused by: (1) Batch effects: Chromosomes on the left image are long and thin but are in contrary on the right image, although they are in the same classes; (2) Inter-class similarity: different classes of chromosomes can be similar in vision such as class 1 and class 2 chromosomes on the two images.

However, all these works are basically taking manually segmented single chromosomes as inputs of classifiers, while clinically all the analysis are based on the entire metaphase image. In this work, we propose a detection based framework, named DeepACC, which not only detect but also fine classify all the 24 class

chromosomes automatically based on the entire metaphase image. As shown in Fig. 1, fine classification of the chromosomes is a challenge task since large intra-class distinctions and small inter-class differences. On the one hand, manual operations and changes of experimental conditions may import **large intra-class distinctions** between different batches of metaphase images, namely batch effects. On the other hand, early seven groups classification criterion [8,19] reveals that different classes of chromosomes within the same group exist **small inter-class differences**. Besides, touching and overlapping of chromosomes on the metaphase images may further bring difficulties for classification. In the following, we enhance the classifier of the model by novelly incorporating the clinical prior knowledge of chromosomes into deep learning models.

Our model is developed based on the Faster R-CNN [18], and the head is separated into two isolated classification stream and regression stream, and then the classification branch is enhanced. We firstly introduce the Additive Angular Margin Loss [3] to enforce higher intra-class compactness and inter-class discrepancy of the model simultaneously. Secondly, as chromosomes usually appear in pairs, we adopt this fact as a prior knowledge and design a siamese structure to **alleviate batch effect** of the metaphase images. Finally, a Group Inner-Adjacency Loss is proposed to take the early grouping criterion of chromosomes [8, 19] as an additional prior knowledge to constraint the network, to further **reduce inter-class similarities** within groups.

2 Method

2.1 Architecture

The goal of this work is to find out all the 24 classes of chromosomes on a metaphase image, which can be served as a multi-class object detection problem. As shown in Fig. 2, we choose the classical object detection framework, Faster R-CNN [18] with backbone network ResNet-101 [7], as our base architecture. Additionally, to identify small chromosomes more accurately, we attach Feature Pyramid Network (FPN) [9] to the backbone network, which combine the high-level information with low-level information together for optimization.

The Region Proposal Network (RPN) [18] is then used to filter out candidate proposals. RPN scans each predefined anchor box for identifying whether the reference box is foreground or background and refining coordinates. Different from the original Faster R-CNN, RoIAlign [6] is introduced to crop features of each candidate proposal. We then divide the detection branch into a classification branch and a regression branch separately in which parameters are not shared. Specifically, the regression branch is consisted by two fully connected layers and constrained by Smooth L1 loss, which is similar to the original Fast R-CNN [5]. Inspired by the visual object tracking model [1], the classification branch is adopted by a siamese architecture which consists two streams sharing two 1024×1024 fully connected layers, the first stream named margin branch optimized by Additive Angular Margin Loss [3] (Section 2.2) and the second stream named inference branch takes the top confident proposal of each class

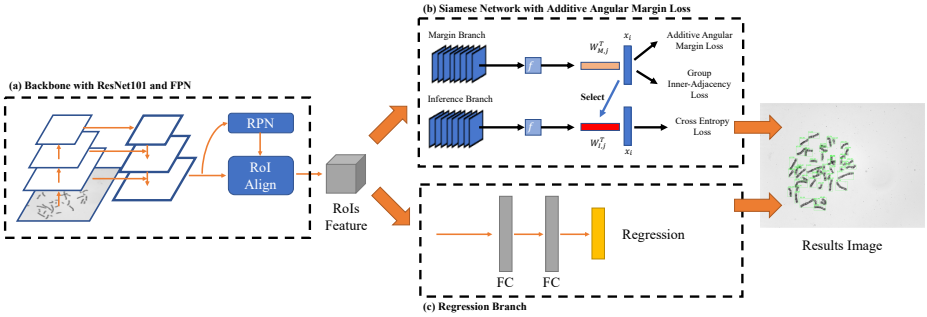

Fig. 2. Architecture of the model, (a) represents backbone network consist of ResNet-101 and FPN, (b)(c) is detection head consists of separately classification branch and regression branch, where (b) shows that siamese network consists of margin and inference branch, with Additive Angular Margin Loss and Group Inner-Adjacency Loss added on. The result is class label of each proposal and its prediction probability.

from the first stream or margin branch weights as local class centers to alleviate batch effects (Section 2.3). Finally, a Group Inner-Adjacency Loss is proposed to further enhance inter-class discrepancy within groups(Section 2.4).

2.2 Margin Branch Enhanced by Additive Angular Margin Loss

It is important to identify the feature differences (e.g. length, banding pattern and centromere index) between different classes of chromosomes. However, the differences between different classes of chromosomes are sometimes tiny but same classes may be in contrary. As a result, we need to obtain higher similarity for intra-class proposals and diversity for inter-class proposals. Inspired by recent research about loss functions of face recognition, we replace the original Cross Entropy (CE) Loss with Additive Angular Margin (AAM) Loss [3].

Similar to the chromosomes classification problem, large-scale face recognition model also need to enhance the discriminative power. Some works [3,11,23] try to achieve above requirements by incorporating margins in an established loss function. In the same way, we reformulate the last fully connected layer of the margin branch without bias term, it can be expressed as $W_j^T x_i = \|W_j\|\|x_i\|\cos\theta_j$, where W_j is j-th column of weight $W \in \mathbb{R}^{d\times n}$ and $x_i \in \mathbb{R}^d$ is the feature of i-th proposal with label y_i. Therefore, W_j can be regarded as representation of j-th class named global class center of j-th class and θ_j represents the angle between global class center W_j and feature x_i. In practice, W_j and x_i is normalized to 1 and rescaled by a scale factor s for easier optimization. An additional margin penalty m is added on each θ_{y_i} to enforce higher intra-class compactness and inter-class discrepancy during training. The formulation of Additive Angular Margin Loss is shown as in Eq. 1:

$$L_{AAM} = -\frac{1}{N}\log\frac{e^{s(\cos(\theta_{y_i}+m))}}{e^{s(\cos(\theta_{y_i}+m))} + \sum_{j\neq y_i, j=1}^{n} e^{s\cos\theta_j}} \tag{1}$$

Comparing to the cross entropy loss, additive angular margin loss directly optimize chromosome feature embeddings to narrow the angle between the same class deep features and broad the angle between different classes.

2.3 Siamese Inference Branch to Alleviate Batch Effect

Besides intrinsic variations between different classes of chromosomes, cytologists may bring in **high intra-class distinctions** between different batches of metaphase images since different operations or conditions, namely batch effects. It is notable that batch effects is inevitable and severe especially in developing countries where most of cytologists are lack of good training. However, batch effects is hard to be learned because of uncertainty of human operation and circumstances. In this work, we try to alleviate batch effects through making full use of local informations on each metaphase image.

As shown in Fig. 3(a)(b), by replacing global class center with the most confident local feature which is more suitable for the specific batch samples, one may obtain a more accurate results and reduce the error, here we name the local feature as local class center. As a well-known prior knowledge, autosomes normally appear as a pair and we may use the most confident chromosome of each class to predict the other one. Practically, including X and Y chromosome, we take the most confident proposal's feature as the local class center of each class to predict the remaining others.

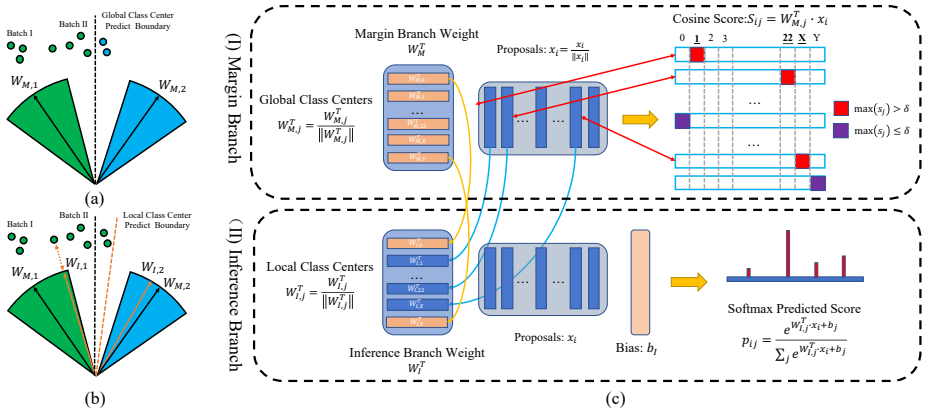

Fig. 3. a) shows predicted results by global class centers $W_{M,1}$ and $W_{M,2}$ which can classify all chromosomes in batch I but misclassify some chromosomes in batch II, (b) Using local class centers $W_{I,1}$ and $W_{I,2}$ can correctly classify all the proposals in batch II. (c) Siamese network architecture which is consist of (I) margin branch and (II) inference branch. Top score proposal of each class which are greater than a given threshold (red rectangles) are selected as local class centers and remaining ones (purple rectangles) are the same as the weights of margin branch.

Inspired by the visual object tracking model [1], we construct a parallel inference branch which yields a siamese architecture together with the margin branch. The two branches share the same input and the margin branch is used to obtain the local class centers which are further adopted as the weights in the inference branch. As illustrated in Fig. 3(c), to obtain weights of inference branch $W_{I,j}$, we firstly find out the most confident proposal x_i of each class j from the margin branch. It is worth noting that some classes of chromosomes may be missing in some cases and local class center may introduce some instability at the beginning stage of the training. Therefore, we set a threshold δ to control where local class center $W_{I,j}$ comes from and normalize them. We finally obtain predict score p_{ij} using the adjusted weights as well as original features without normalization and constrain it by a cross entropy(CE) loss:

$$W_{I,j} = \begin{cases} \dfrac{x_i}{\|x_i\|}, & s_{\arg\max_i s_{ij},j} > \delta \\ \dfrac{W_{M,j}}{\|W_{M,j}\|}, & s_{\arg\max_i s_{ij},j} \leq \delta \end{cases}, \quad p_{ij} = \frac{e^{W_{I,j}^T \cdot x_i + b_j}}{\sum_j e^{W_{I,j}^T \cdot x_i + b_j}} \tag{2}$$

where b_j is a bias term initialized as constant zero. The scores obtained in the inference branch are regarded as the final predicted results.

Remark: By keeping the bias term and constraining by CE loss, the inference branch not only takes the advantage of discriminative power bringing by the AAM loss and optimized decision boundaries which reduce batch effects, but also avoids information loss due to feature normalization and flexibility reduction due to the lack of bias terms (as pointed in [22] for L_{AAM}).

2.4 Group Inner-Adjacency Loss Using Prior Knowledge

Besides classical 24 classes criterion, cytologists generally agreed that chromosomes also can be classified to seven groups according to the size and centromeric index, including group $\mathcal{G}_A$ (chromosome 1-3), $\mathcal{G}_B$ (chromosome 4-5), $\mathcal{G}_C$ (chromosome 6-12, X), $\mathcal{G}_D$ (chromosome 13-15), $\mathcal{G}_E$ (chromosome 16-18), $\mathcal{G}_F$ (chromosome 19-20) and $\mathcal{G}_G$ (chromosome 21-22, Y), namely Denver System [8, 19]. Though it is an empirical criterion, it somehow indicates that **inter-class similarities** within groups is more severe and need to take special care of. Therefore, inspired by the Non-Adjacency Loss [4], we take the clinically seven group criterion as a prior knowledge, and propose an additional group inner-adjacency loss to further optimize class discriminability of the model within each group.

Defining two different classes as adjacent if they belong to the same group, and a set of forbidden group inner-adjacency class $\mathcal{F} = \{(i,j)|i \in \mathcal{G}_k, j \in \mathcal{G}_k, i \neq j, k \in \{A,B,C,D,E,F,G\}\}$. For each positive proposal x_i with label y_i, the probability of x_i belonging to its forbidden group inner-adjacency class j should be null. To this end, let $M(x_i)$ be the probability vector of x_i from the margin branch and $M_j(x)$ be the probability vector of the top confident proposal of its adjacent class j, we enforce $M(x_i) \cdot M_j(x)$ to be low until two vectors are vertical in geometry space. In practice, the group inner-adjacency loss is designed

to minimize the sum of element-wise product of the probability vectors between y_i and its forbidden group inner-adjacency class j where $(y_i, j) \in \mathcal{F}$:

$$L_{GIA}(x) = \frac{1}{N_+} \sum_{i}^{N_+} \sum_{(y_i,j)\in\mathcal{F}}^{N_{(y_i,j)}} M(x_i) \cdot M_j(x) \tag{3}$$

Here, $N_{(y_i,j)}$ is the number of group inner-adjacency classes of class y_i and N_+ is the number of positive proposals.

3 Experiments

3.1 Dataset and Implementation Details

We collect 3390 Giemsa-stained metaphase images with 1600×1200 resolution from clinical cytogenetics laboratory, where each chromosome is labelled with a bounding box and its class by experienced cytologists. The dataset is divided into 3(2034) : 1(678) : 1(678) as training, validation and testing set. All images are normalized by mean and standard deviation. During training, only random ($p = 0.5$) horizontally flipping are used for data augmentation. DeepACC is end-to-end jointly optimized by the loss detailed as following:

$$L = L_{det} + \alpha L_{AAM} + \beta L_{CE} + \gamma L_{GIA} \tag{4}$$

Here L_{det} indicates the original Faster R-CNN loss except for classification head. In all experiments, we set α as 0.1, β as 1.0 and γ as 0.1. The margin penalty m and scale factor s used in Additive Angular Margin Loss L_{AAM} are set as 0.25 and 64 respectively. All the remaining settings are the same as Faster R-CNN.

The classical mean Average Precision (mAP) is adopted to evaluate the performance of the model. However, since in practice we only take Top 1 score class of each example into account for classification problem, we also introduce an mAP_{max} as an evaluation metric, which only take the Top 1 score bounding box of each proposal to compute mAP. Furthermore, since clinically cytologists pay more attention on proposals at high score (here we set threshold as $p \geq 0.5$), we ignore low-score proposals and further reduce redundancy by class-agnostic NMS (0.7 threshold) after Top 1 score bounding box selection, and then introduce Accuracy (Acc) and Average Error Ratio (AER) to evaluate the performance. Acc is defined as proportion of true positive in all predictions and AER is defined as the fraction of sum of false positives and false negatives divided by the number of ground truth. The definitions of true positive, false positive and false negative are the same as DeepACE [24].

The model is implemented on MMDetection [2] toolbox that based on Pytorch [15] framework. We set batch size as 1 and trained the network for 24 epochs with 0.02 initial learning rate which is decayed by a factor of 10 at 16 and 22 epoch. Stochastic Gradient Descent (SGD) is adopted to optimize our network on a Nvidia Titan Xp GPU with momentum= 0.9.

3.2 Ablation Study

Ablation studies are performed on the validation set to test the effect of each individual module proposed in our model and summarized in Table 1. We also test and explore that simply separating classification and regression branch does not improve the performance (Table 1(a)(b)).

As shown in Table 1(e), combination of Additive Angular Margin Loss and Siamese Inference Branch can have significant improvements on all metrics, where mAP(%) over baseline by 0.46, mAP$_{max}$(%) by 1.03, AER(%) by 1.53 and Acc(%) by 1.22. Specifically, it is worth noting that adding Additive Angular Margin Loss only (Table 1(c)) can deteriorate the performance at some extent, this may because that the lack of bias term as well as feature normalization in L_{AAM} can destroy the discrimination ability of specific class (as pointed in [22]). However, more compact and well-separated features obtained from the L_{AAM} can still help Siamese Inference Branch selects more representative local class centers to reduce batch effects (Table 1(d)(e)). In addition, adding the Group Inner-Adjacency Loss (Table 1(f)) can further reduce the misclassification error within groups and improve the performance.

Table 1. Ablation study on validation set, where sep means isolated classification and regression branch. L_{AAM} means Additive Angular Margin Loss, Siamese means siamese inference branch and L_{GIA} means Group Inner-Adjacency Loss.

Method	L_{AAM}	Siamese	L_{GIA}	mAP(%)	mAP$_{max}$(%)	AER(%)	Acc(%)
(a)Faster R-CNN				90.82	88.10	18.09	83.34
(b)Faster R-CNN(sep)				90.89	88.23	18.09	83.33
(c)DeepACC	✓			87.76	87.23	17.64	83.80
(d)DeepACC		✓		91.24	88.63	17.73	83.56
(e)DeepACC	✓	✓		91.28	89.13	16.56	84.56
(f)DeepACC	✓	✓	✓	**91.43**	**89.38**	**16.22**	**84.85**

3.3 Main Results

Final results are reported in Table 2, we compare our proposed model with two-stage object detection baseline, Faster R-CNN and one-stage object detection baseline, RetinaNet. All experiments are trained with combination of training and validation set and final results are reported based on the testing set. DeepACC greatly outperforms both of the baselines, achieving an mAP(%) of 91.88, mAP$_{max}$(%) of 89.80, AER(%) of 15.45 and Acc(%) of 85.54.

Table 2. Final results on testing set.

Method	Backbone	Neck	mAP(%)	mAP$_{max}$(%)	AER(%)	Acc(%)
RetinaNet [10]	ResNet-101	FPN	91.31	88.57	19.74	82.00
Faster R-CNN [18]			91.60	88.97	16.84	84.40
DeepACC			**91.88**	**89.80**	**15.45**	**85.54**

4 Conclusion

This work creatively proposed a detection based deep learning model to detect and fine classify chromosomes from entire metaphase image. After introducing the Additive Angular Margin Loss to enhance the discriminative power, a siamese inference branch is proposed to transform decision boundary of each class by making full use of prior knowledges that chromosomes usually appear in pairs. In addition, clinical grouping criterion is taken as a prior knowledge to further reduce classification errors within groups. The DeepACC significantly outperforms both the state-of-the-art two-stage and one-stage baselines.

5 Acknowledgement

This work was supported by National Natural Science Foundation of China(grant 31900979) to Li Xiao.

6 Author Contributions

Tianqi Yu, Manqing Wang, Fuhai Yu, Chan Tian, and Jie Qiao collected and labeled the data. Chunlong Luo, Li Xiao, Yufan Luo, and Yinhao Li designed the model and analyzed the data. Chunlong Luo implemented the model. Li Xiao conceived and supervised this work and wrote the manuscript with assistance from Jie Qiao and Chan Tian. Further information or questions should be directed to the Lead Contact, Li Xiao (xiaoli@ict.ac.cn).

References

1. Bertinetto, L., Valmadre, J., Henriques, J.F., Vedaldi, A., Torr, P.H.: Fully-convolutional siamese networks for object tracking. In: European conference on computer vision. pp. 850–865. Springer (2016)
2. Chen, K., Wang, J., Pang, J., Cao, Y., Xiong, Y., Li, X., Sun, S., Feng, W., Liu, Z., Xu, J., Zhang, Z., Cheng, D., Zhu, C., Cheng, T., Zhao, Q., Li, B., Lu, X., Zhu, R., Wu, Y., Dai, J., Wang, J., Shi, J., Ouyang, W., Loy, C.C., Lin, D.: MMDetection: Open mmlab detection toolbox and benchmark. arXiv preprint arXiv:1906.07155 (2019)
3. Deng, J., Guo, J., Xue, N., Zafeiriou, S.: Arcface: Additive angular margin loss for deep face recognition. In: Proceedings of the IEEE Conference on Computer Vision and Pattern Recognition. pp. 4690–4699 (2019)
4. Ganaye, P.A., Sdika, M., Triggs, B., Benoit-Cattin, H.: Removing segmentation inconsistencies with semi-supervised non-adjacency constraint. Medical image analysis **58**, 101551 (2019)
5. Girshick, R.: Fast r-cnn. In: Proceedings of the IEEE international conference on computer vision. pp. 1440–1448 (2015)
6. He, K., Gkioxari, G., Dollár, P., Girshick, R.: Mask r-cnn. In: Computer Vision (ICCV), 2017 IEEE International Conference on. pp. 2980–2988. IEEE (2017)

7. He, K., Zhang, X., Ren, S., Sun, J.: Deep residual learning for image recognition. In: Proceedings of the IEEE conference on computer vision and pattern recognition. pp. 770–778 (2016)
8. Lejeune, J., Levan, A., Böök, J., Chu, E., Ford, C., Fraccaro, M., Harnden, D., Hsu, T., Hungerford, D., Jacobs, P., et al.: A proposed standard system of nomenclature of human mitotic chromosomes. The Lancet **275**(7133), 1063–1065 (1960)
9. Lin, T., Dollár, P., Girshick, R.B., He, K., Hariharan, B., Belongie, S.J.: Feature pyramid networks for object detection. In: 2017 IEEE Conference on Computer Vision and Pattern Recognition, CVPR 2017, Honolulu, HI, USA, July 21-26, 2017. pp. 936–944 (2017)
10. Lin, T.Y., Goyal, P., Girshick, R., He, K., Dollár, P.: Focal loss for dense object detection. In: Proceedings of the IEEE international conference on computer vision. pp. 2980–2988 (2017)
11. Liu, W., Wen, Y., Yu, Z., Li, M., Raj, B., Song, L.: Sphereface: Deep hypersphere embedding for face recognition. In: Proceedings of the IEEE conference on computer vision and pattern recognition. pp. 212–220 (2017)
12. Markou, C., Maramis, C., Delopoulos, A., Daiou, C., Lambropoulos, A.: Automatic chromosome classification using support vector machines. Google Scholar pp. 1–24 (2012)
13. Ming, D., Tian, J.: Automatic pattern extraction and classification for chromosome images. Journal of Infrared, Millimeter, and Terahertz Waves **31**(7), 866–877 (2010)
14. Nair, R.M., Remya, R., Sabeena, K.: Karyotyping techniques of chromosomes: a survey. Int J Comput Trends Technol **22**(1) (2015)
15. Paszke, A., Gross, S., Massa, F., Lerer, A., Bradbury, J., Chanan, G., Killeen, T., Lin, Z., Gimelshein, N., Antiga, L., et al.: Pytorch: An imperative style, high-performance deep learning library. In: Advances in Neural Information Processing Systems. pp. 8024–8035 (2019)
16. Patterson, D.: Molecular genetic analysis of down syndrome. Human genetics **126**(1), 195–214 (2009)
17. Qin, Y., Wen, J., Zheng, H., Huang, X., Yang, J., Song, N., Zhu, Y.M., Wu, L., Yang, G.Z.: Varifocal-net: A chromosome classification approach using deep convolutional networks. IEEE transactions on medical imaging **38**(11), 2569–2581 (2019)
18. Ren, S., He, K., Girshick, R., Sun, J.: Faster r-cnn: Towards real-time object detection with region proposal networks. In: Advances in neural information processing systems. pp. 91–99 (2015)
19. Schmid, W., Atkins, L., Böök, J., Gustavson, K.H., Hansson, O., Hjelm, M., Ohno, S., Jainchill, J., Stenius, C., Hamerton, J., et al.: The london conference on the normal human karyotype. Cytogenetic and Genome Research **2**(4-5), 264–268 (1963)
20. Sharma, M., Saha, O., Sriraman, A., Hebbalaguppe, R., Vig, L., Karande, S.: Crowdsourcing for chromosome segmentation and deep classification. In: 2017 IEEE Conference on Computer Vision and Pattern Recognition Workshops (CVPRW). pp. 786–793 (July 2017)
21. Swati, Gupta, G., Yadav, M., Sharma, M., Vig, L.: Siamese networks for chromosome classification. In: 2017 IEEE International Conference on Computer Vision Workshops (ICCVW). pp. 72–81 (Oct 2017)
22. Wang, F., Xiang, X., Cheng, J., Yuille, A.L.: Normface: L2 hypersphere embedding for face verification. In: Proceedings of the 25th ACM international conference on Multimedia. pp. 1041–1049 (2017)
23. Wang, H., Wang, Y., Zhou, Z., Ji, X., Gong, D., Zhou, J., Li, Z., Liu, W.: Cosface: Large margin cosine loss for deep face recognition. In: Proceedings of the IEEE Conference on Computer Vision and Pattern Recognition. pp. 5265–5274 (2018)

24. Xiao, L., Luo, C., Luo, Y., Yu, T., Tian, C., Qiao, J., Zhao, Y.: Deepace: Automated chromosome enumeration in metaphase cell images using deep convolutional neural networks. In: International Conference on Medical Image Computing and Computer-Assisted Intervention. pp. 595–603. Springer (2019)